ACS Photonics

pubs.acs.org/journal/apchd5 Article

Steering of Guided Light with Dielectric Nanoantennas

Ivan Sinev,* Filipp Komissarenko, Ivan Iorsh, Dmitry Permyakov, Anton Samusev, and Andrey Bogdanov

Cite This: ACS Photonics 2020, 7, 680−686 Read Online

ACCESS | Metrics & More | Article Recommendations | Supporting Information

ABSTRACT: All-dielectric nanoantennas proved to be an extremely versatile tool for efficient light manipulation at the nanoscale. Their rich functionality and excellent performance arise due to low absorption and high refractive index of all-dielectric materials, in particular, silicon, which enables the observation of pronounced magnetic and electric Mie resonances in subwavelength structures in the visible and near-infrared ranges. Here, we demonstrate that all-dielectric spherical nanoantennas placed on a substrate supporting guided modes provide efficient control over their directivity pattern, achieved due to the interplay between polarization of the incident light and the interference of electric and magnetic dipole resonances of the nanoantenna. In particular, by managing only the wavelength and polarization state of the incident plane wave at a fixed direction of incidence, it is possible to implement highly directional full-angle steering of surface plasmon polariton on a gold film. As a proof of concept, we experimentally demonstrate plasmonic beam steering with a single silicon nanoantenna using circular polarization of light. Our approach offers unprecedented versatility for designing nanoscale antennas with applications in integrated nanophotonics and quantum optics.

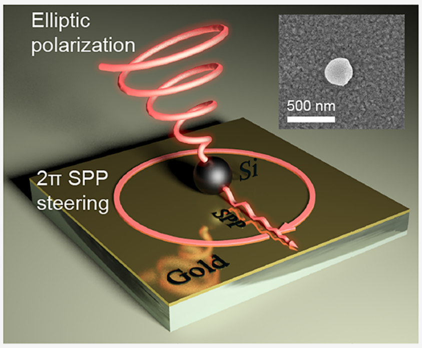

KEYWORDS: *all-dielectric nanoantennas, surface plasmon polaritons, directional scattering, silicon, magnetic dipole resonance, leakage radiation microscopy*

All-dielectric structures made of high refractive index materials have firmly established themselves as a most efficient tool for light manipulation at the nanoscale.[1−4] The main concept underlying the unique properties of high-index dielectric nanoantennas and metasurfaces is the combination of strong magnetic and electric resonances that could be observed in the visible and infrared spectral ranges.[5] Low material losses and readily available frequency scaling of these resonances in dielectric structures give them an important advantage over plasmonic structures. Moreover, dielectric Mie resonances can provide extremely strong field localization that can be used for enhanced light−matter interaction and nonlinear optics.[6−8]

Strong magnetic optical resonance provides an essential degree of freedom that enables efficient manipulation of scattering from individual dielectric particles and their arrays. In particular, it inspired all-dielectric-based designs for single nanoantennas with suppressed backscattering of light (Kerker regime),[9,10] and Huygens metasurfaces.[11] With higher order multipoles coming into play, dielectric nanoantennas offer precise control of the directivity patterns[12] and enable strong suppression of far-field scattering (anapole regime).[13,14]

Naturally, all-dielectric nanoantennas can also be used for directional excitation of guided modes and manipulation of their directivity patterns.[15,16] The idea is based on one of the key properties of guided light, with its intrinsic transverse spin angular momentum locked with the propagation direction.[17] The transverse spin angular momentum is the general property of any near field, which inherently has a spinning structure and can be efficiently coupled to a spinning dipole. The directivity of guided light excitation strongly depends on the handedness of the spinning dipole.[18,19] This phenomenon is often called optical spin Hall effect.[20,21] Since the first demonstrations of unidirectional launching of surface plasmon polaritons (SPP) from a slit in a metal film under circularly polarized light excitation,[22,23] this effect has found numerous applications in the fields from integrated nanophotonics to quantum optics[24] and optomechanics.[25] New fascinating physics is still discovered both in far-field and near-field radiation patterns of dipole sources.[26−29]

Latest research revealed that directional excitation of guided light spans beyond the well-known locking of spinning sources with the spin of the guided mode when magnetic response comes into play. Namely, near-field interference of magnetic and electric dipole modes can also lead to directional excitation of surface waves and guided modes,[15,16] which is a special case of a more general phenomenon of directional emission and scattering of light that is observed in a wide range of systems.[10,30,31] Alternatively, directional scattering of light is also achieved through more complex engineering of the local polarization state of the incident wave.[32,33]

Received: October 16, 2019
Published: February 4, 2020

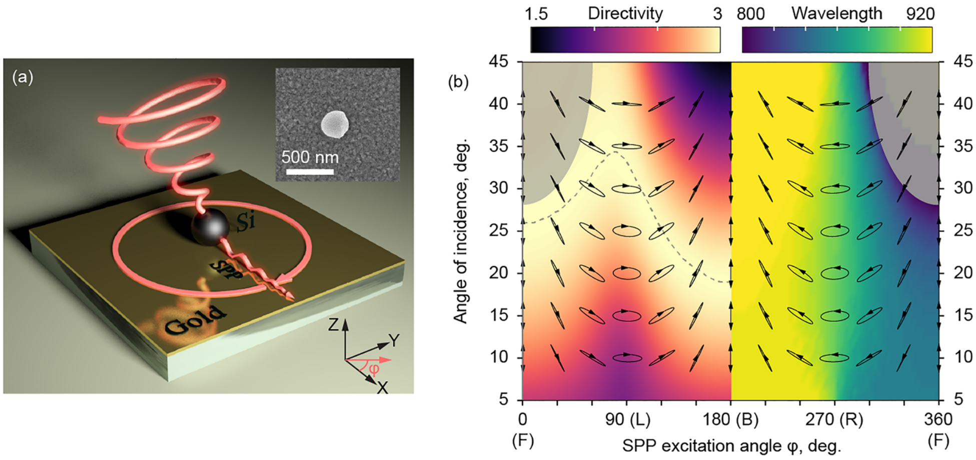

Figure 1. (a) Illustration of the concept of plasmonic beam steering with silicon nanoantenna. (b) Map of the analytically calculated SPP directivity from a 295 nm silicon nanosphere that can be achieved for all azimuthal angles of SPP excitation φ, see the scheme in (a), and for different angles of incidence θ by controlling the wavelength and polarization state of light. Left part of the map shows the dependence of the directivity value on θ and φ, the right part shows the excitation wavelength required to achieve the respective directivity (both maps are symmetric with respect to φ = 180 axis, i.e., wavelength and directivity are the same for φ = 90 and 270). The overlay shows the polarization states of the incident light that provide the optimal directivity values. Gray-shaded areas represent the geometries when maximum directivity is achieved beyond the boundaries of the considered spectral range (800−1100 nm). Dashed line tracks the conditions when the directivity reaches the value of 3.

The important drawback of using dipolar nanoantennas for light manipulation is the constraint on the maximum directivity of the scattered wave, which does not exceed 3 both for bulk and surface waves.[15,34] However, such directivity is not easy to obtain, even in a single direction. For surface waves, practical realizations of near-field coupling are usually limited to bidirectional (left/right, forward/backward) operation.[23] Recently, we showed that a single silicon nanoantenna can provide switching of surface plasmon polaritons with forward and backward directivities achieving the maximum value of 3 within a narrow spectral band.[15] However, full angular control over the guided mode excitation direction, to the best of our knowledge, has not yet been demonstrated.

Here, we show that full 2π steering of SPP from a single high-index dielectric nanoantenna can be achieved by combining and independently controlling the interference of electric and magnetic dipole moments of the nanoantenna induced by the obliquely incident elliptically polarized light. While the longitudinal (forward/backward) switching of SPP is defined by the relative phase and amplitude of magnetic and electric dipole responses of the nanoantenna that is arranged through changing the wavelength, the helicity of the excitation wave introduces the asymmetry with respect to the plane of incidence that the system initially lacks. Thus, by controlling the wavelength and the polarization state of incident light simultaneously, the resulting surface wave generated by the nanoantenna can be bent to the desired direction. Namely, the SPP on a gold film can be excited by a silicon nanosphere in any direction with the directivity of 3 (maximum achievable for an antenna with only dipole polarizabilities), which provides a decisive advantage over previously reported designs of antennas for SPP. In the experiment, we demonstrate plasmonic beam steering from a single silicon nanosphere on gold using only circular polarization of the incident light.

METHODS

The calculations of the directivity patterns of SPP from a single silicon nanosphere on gold excited by plane waves with different polarization states were performed analytically using Green's function approach[15,35] and independently checked with simulations in a COMSOL Multiphysics package.

During the substrate preparation, a thin (2 nm) adhesion layer of chromium, followed by a 40 nm layer of gold, were thermally evaporated on a glass substrate. The gold thickness was chosen to ensure sufficient leakage radiation of SPP without the perturbation of the SPP dispersion as compared to a bulk gold substrate. Silicon nanospheres were fabricated using a laser ablation technique[36] and subsequently transferred on gold films using nanomanipulations under electron beam supervision.[37,38]

To measure the SPP directivity patterns experimentally, we used a leakage radiation microscopy setup combined with Fourier plane imaging optics. Single silicon nanosphere on thin gold film was excited with mildly focused laser beam with tunable wavelength provided by spectrally filtered supercontinuum laser source (Fianium WhiteLase with acousto-optical tunable filter). The polarization state of light was controlled with a linear polarizer (Glan-Taylor prism) and a broadband achromatic quarter-waveplate (Thorlabs). Transmitted light and SPP leakage radiation were collected with an oil immersion objective (Zeiss 100× NA = 1.42). Both direct and Fourier images were recorded with separate cameras. In the Fourier image channel, the directly transmitted radiation was attenuated with a circular beam block positioned in the intermediate Fourier plane of the optical setup.

RESULTS

SPP from a Dielectric Nanoantenna. The directivity pattern of a surface plasmon polariton excited with an all-dielectric nanoantenna can be calculated analytically using a Green's function approach, where the nanoantenna is treated as a point dipole with electric and magnetic polarizabilities.[15,35] Starting with the calculation of these polarizabilities with an account for the gold substrate, we proceed to obtain the full electric and magnetic dipole moments induced in the nanoparticle for a given polarization state and angle of

https://dx.doi.org/10.1021/acsphotonics.9b01515
ACS Photonics 2020, 7, 680−686

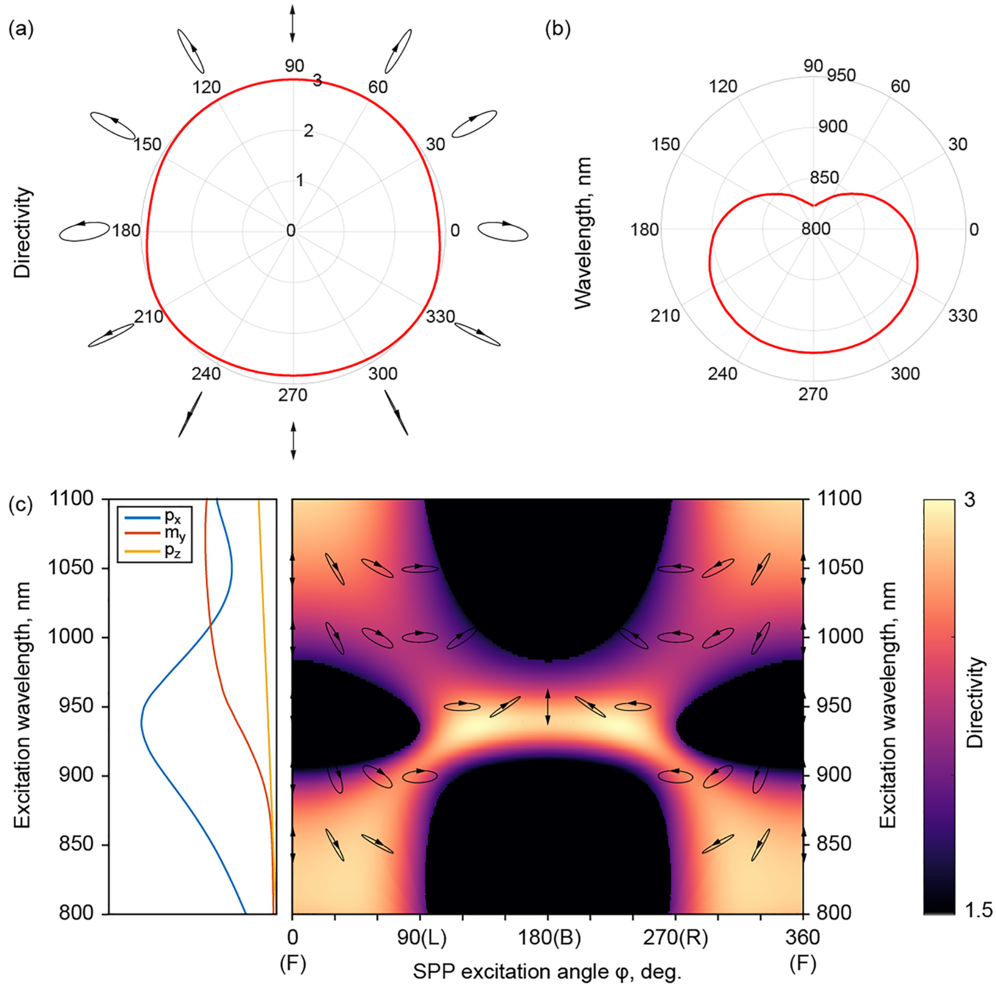

Figure 2. (a, b) Diagrams illustrating the conditions for achieving maximum directivity of surface plasmon polariton from a 295 nm silicon nanosphere on gold for AOI = 25°. (a) Maximum directivity diagram. Polarization states of incident light allowing maximum directivity are marked for characteristic angles. (b) Diagram indicating the wavelengths at which the maximum directivity is achieved for each in-plane angle. (c) Polarization-only tuning of the directivity pattern: map of the maximum SPP directivity achieved for AOI = 25°, only by changing the polarization state of the incident light for fixed wavelengths. The left panel shows the spectral dependence of the dipole components induced in the nanosphere for TM-polarized incident light.

incidence (AOI) of the excitation wave (see Supporting Information, section 1, for the calculation details). The dependence of the intensity I_{SPP} of the surface plasmon polariton excited by the induced dipole moments on the azimuthal angle φ is given by the following equation:[15]

$$I_{SPP}(\varphi) \sim |\underbrace{(m_x + i\kappa p_y)\sin\varphi}_{\text{from TE wave}} + \underbrace{(m_y - i\kappa p_x)\cos\varphi - \tilde{k}_{SPP}p_z}_{\text{from TM wave}}|^2 \quad (1)$$

where m_i and p_i are the Cartesian components of the induced magnetic and electric dipole moments, respectively, the z axis is the normal to the substrate, and the plane of incidence is the xz one. $\tilde{k}_{SPP}$ and κ stand for the normalized SPP wave vector components: $\tilde{k}_{SPP} = k_{SPP}/k_0 = \sqrt{\varepsilon_m/(\varepsilon_m + 1)}$ and $\kappa = -i\tilde{k}_z = -i\sqrt{1 - \tilde{k}_{SPP}^2} = -i\sqrt{1/(\varepsilon_m + 1)}$. For the case of TM-polarized excitation, eq 1 reveals the conditions for suppression of backward and forward scattering of SPP: $(m_y - i\kappa p_x)/(\tilde{k}_{SPP}p_z) = \pm 1$. These conditions can be considered as an extension of the first and second Kerker conditions[39] to the domain of surface waves.[15] It follows from eq 1 that independent excitation of SPP with TE- or TM-polarized waves results in radiative patterns that are symmetric with respect to the plane of incidence (see Supporting Information, Figure S3). To provide this kind of asymmetry, the incident wave should contain both the TE- and TM-components of the incident field. Indeed, considering eq 1 for $\varphi = \pm\pi/2$, one can note that zero left/right SPP excitation can be achieved for arbitrary nonzero polarizability components of the nanoparticle by controlling the polarization state of the incident light (that is, the relative amplitudes and phases of TE- and TM-components of the incident field). This indicates the possibility of plasmonic beam steering with a single dielectric nanoantenna, since the control of TE/TM ratio of the incident light can be combined with forward/backward SPP switching available through wavelength tuning (see the general scheme in Figure 1a).

However, the problem of finding the application-relevant conditions for maximum SPP directivity in a particular direction is not that straightforward. While it can be done through taking the second angle derivative of the expression for the SPP intensity, the resulting expressions are too cumbersome for a feasible analysis. Therefore, to explore the ultimate capabilities of SPP steering with a silicon nanoantenna, we address the full "wavelength - polarization state - angle of incidence" parameter space analytically to find the conditions that allow to achieve the maximum directivity for each angle of SPP excitation within the substrate plane. Without the loss of generality, henceforth, we study a 295 nm silicon nanosphere on gold substrate within 800 to 1100 nm spectral region where the optical response of such sphere is dominated by the dipolar components of its polarizability. The functionality that we discuss, however, can be easily extended to other spectral regions due to the scalability of the resonances of high-index dielectric nanoantennas.[1,2,15]

Figure 1b combines the SPP directivity data calculated for a 295 nm silicon nanosphere on gold for angles of incidence from 5° to 45°. In the left part of the panel, each point of the map represents the maximum SPP directivity from the nanoantenna that can be achieved for the given angle of incidence θ (vertical axis) and azimuthal angle φ, measured with respect to the projection of the incident wavevector on the substrate surface, horizontal axis) by tuning the polarization state and wavelength (within 800−1100 nm spectral range) of the incident wave. The right part of the panel shows the wavelength of the incident light that is required to achieve the respective directivity value. Note that for two directions symmetric with respect to the plane of incidence (e.g., $\varphi = 90°$ and 270°), both the maximum directivity and the required wavelength are the same, and the only thing that changes is the polarization state. The data analysis reveals that, in an analytical calculation, within the chosen parameter space the maximum directivity (which is 3 since we consider dipole approximation) can be achieved for any desired φ, as shown with dashed line. For four characteristic directions (forward, backward, right/left), upon increasing the angle of incidence, the maximum directivity is first reached for backward direction (18°), followed by the forward direction at 25°. Finally, for the left/right direction, the maximum is achieved at around 32°. The results of analytical modeling are in good agreement with numerical calculation (see Supporting Information, Figure S2); however, the maximum directivity for the latter is achieved for slightly higher angles of incidence. We attribute this fact to the influence of the strong near-field associated with a p_z dipole moment, which is not fully accounted for in point dipole approximation of the analytical approach.

As it appears, highly directional steering of SPP is possible even without changing the angle of incidence. As an example, the section of Figure 1b for AOI = 25° (analytical model) is shown in Figure 2a. For this excitation geometry, resonant silicon nanoparticle provides highly directive excitation of SPP (directivity $D > 2.8$) for any azimuthal angle φ. The polarization state required for optimal directivity values evolves from p-polarization for forward excitation ($\varphi = 90°$) to elliptical for left and right directions and back to p-polarization for backward excitation regime, as illustrated by polarization ellipses in Figure 2a. As mentioned before, achieving optimal directivity also requires simultaneous tuning of the excitation wavelength, as shown in Figure 2b. It reveals that the beam steering effect is observed within a narrow range of wavelengths between electric and magnetic dipole resonances of the particle (Figure 2b) that corresponds to the spectral region of front-to-back switching of SPP for p-polarized excitation reported in our earlier work.[15] The SPP steering in numerical simulation for a single angle of incidence is also illustrated in Supporting Information, Movie S1. Calculations of the cross section of scattering into SPP reveal that the excitation efficiency is the highest for forward and backward directions and drops toward left/right excitation directions. In particular, for angle of incidence of 25 degrees the SPP excitation cross section varies within 0.15−0.6 of the geometrical section of the particle depending on the SPP excitation direction. The description of the calculation routine as well as the map of SPP excitation efficiency for different θ and φ can be found in Supporting Information, sections 4 and 5.

Without the change of wavelength, the SPP steering for silicon nanoantenna is limited both in maximum achievable directivity and the range of available excitation directions. This is illustrated in Figure 2c, where for each wavelength within 800−1100 nm spectral range, we plot the maximum SPP directivity that can be achieved for all φ by changing the polarization state of the incident light (here, AOI = 25° is considered as well). For a single wavelength, the steering range is limited to <180°, as the possibility of tuning the interference conditions of magnetic and electric dipoles is disabled.

Experiment. To demonstrate the concept of plasmonic beam steering experimentally, we visualize the directivity patterns of SPP from a silicon nanosphere on gold with leakage radiation microscopy setup.[15] The experimental scheme is illustrated in Figure 3. Due to a dramatic dependence of the

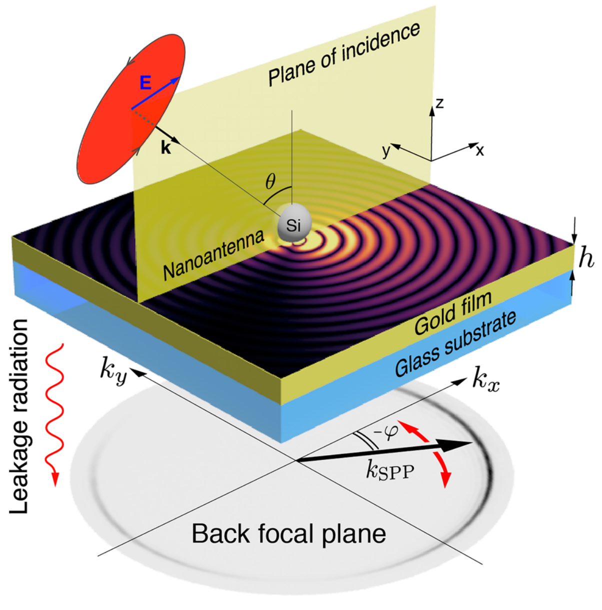

Figure 3. Schematic of the SPP directivity measurement. SPP leakage radiation is collected with an immersion objective and imaged in the back focal plane of the setup to visualize its angular spectrum.

phase of the induced dipole moments on the wavelength (see Supporting Information, Figure S1b), the conditions for optimal directivity can be modified even by slight shape imperfections of the silicon nanosphere that add the effect of geometrical chirality of the nanoparticle to the scene. Therefore, the conditions for optimal directivity in a particular direction may deviate from those predicted by the analytical model. In practice, this means that finding the polarization state required for maximum directivity in all directions would

https://dx.doi.org/10.1021/acsphotonics.9b01515
ACS Photonics 2020, 7, 680−686

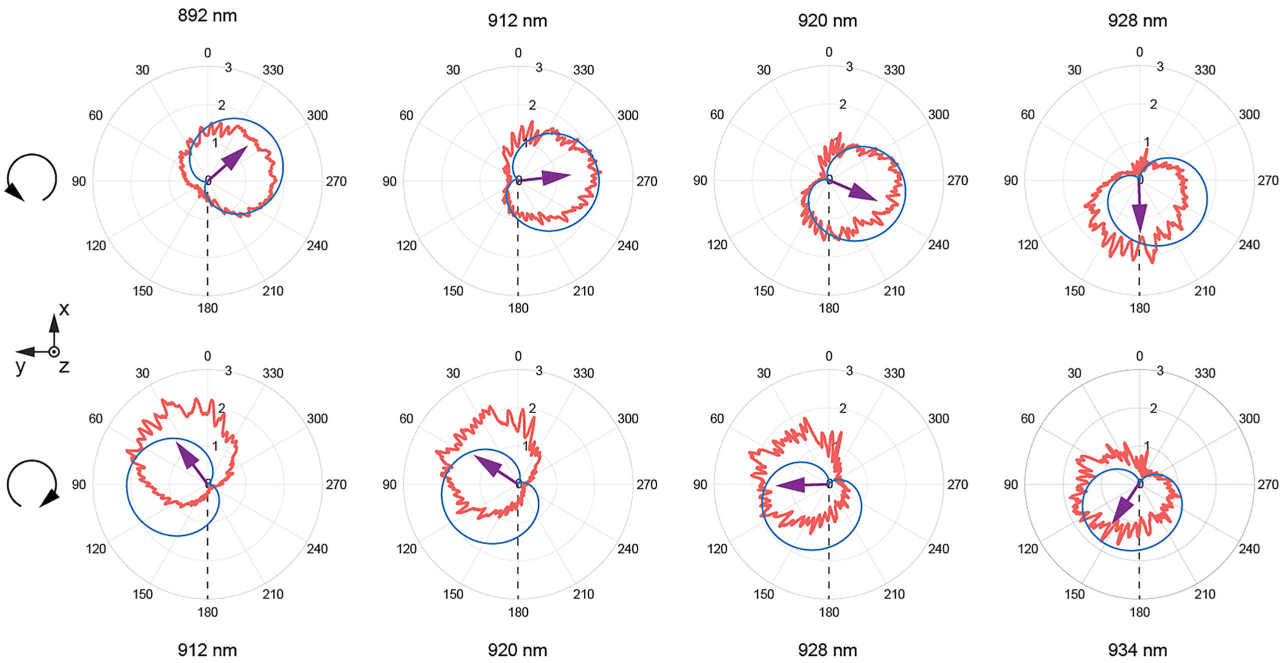

Figure 4. SPP directivity diagrams illustrating plasmonic beam steering effect achieved using circularly polarized light excitation (25 degrees AOI) of both helicities: left (top row) and right (bottom row). The experimental directivity patterns reconstructed from the back focal plane images are shown with red lines. Gray dashed line denotes the excitation direction, arrows illustrating the approximate direction of SPP excitation are added as a guide for the eye. Blue lines represent the numerical calculation of the directivity patterns. Slight lagging of the numerical pattern with respect to the experiment for RCP is attributed to the shape imperfections of the nanoparticle.

force one to sweep through multiple polarization states, making the experiment extremely time-consuming. Here, we focus on demonstrating the steering effect for left/right circular polarization. Remarkably, even a single polarization state provides a vivid beam steering effect upon changing the wavelength of the incident beam between electric and magnetic dipole resonances of the nanosphere.

The experimental results measured for circularly polarized excitation incident at 25° on a 295 nm silicon nanosphere on gold are shown in Figure 4. Solid red lines show the SPP directivity patterns reconstructed from the Fourier plane images of the SPP leakage radiation for left and right circularly polarized (LCP/RCP) excitation. By controlling the helicity of the incident light as well as its wavelength, we are able to achieve almost 2π steering effect as the directivity patterns evolve from right- to left-oriented (with respect to the incident beam) within the spectral band of less than 50 nm. The SPP directivity patterns calculated analytically are shown in the same figure with blue lines. As mentioned above, the comparison of the experimental and analytical patterns is hindered by the slight asymmetry of the nanoparticle (see also the inset in Figure 1a). This leads to the lack of symmetry of the experimentally measured steering pattern upon switching from right to left circularly polarized excitation and subsequent “lagging” of the numerical directivity patterns as compared to the experiment (bottom row in Figure 4).

The observed steering effect highlights the combined action of the interference of magnetic and electric dipole moments of the nanoparticle with helicity of the incident wave and constitutes a striking difference with previously reported results,[18,23,40] where the helicity of incident light exclusively determined the direction of excitation of surface waves. The full spectral dependence of the measured directivity patterns for both circular polarizations illustrating the rotation of the directivity pattern with the change of the wavelength can be found in the Supporting Information, Movies S2 and S3. The observed rapid change of the excitation direction with the wavelength detuning suggests new applications for tunable SPP nanoantennas employing nonlinear effects[41] or based on phase change materials[42] or liquid crystals.[43]

■ CONCLUSION

To conclude, we have demonstrated extremely high versatility of high-index dielectric nanoantennas as directional sources for surface waves. We showed that the combined action of the interference of electric and magnetic dipole resonances of the particle and polarization state of the incident wave enables full control over direction of excitation of guided light from the nanoantenna. While here we showcased the steering effect for surface plasmon polaritons from a single silicon nanoantenna, the same concept can be extended to other types of guided waves, such as modes of planar waveguides and photonic crystal slabs. This establishes new opportunities for the design of flexible nanoscale sources and management of signal transfer.

■ ASSOCIATED CONTENT

Supporting Information

The Supporting Information is available free of charge at https://pubs.acs.org/doi/10.1021/acsphotonics.9b01515.

Additional calculations of silicon nanosphere polarizability components and conditions for achieving maximum directivity. Comparison of numerical and analytical calculations and calculations of the SPP excitation efficiency (PDF)

Movie S1 (AVI)
Movie S2 (AVI)
Movie S3 (AVI)

AUTHOR INFORMATION

Corresponding Author

Ivan Sinev − *Department of Physics and Engineering, ITMO University, St. Petersburg, Russia*; orcid.org/0000-0002-4246-7747; Email: i.sinev@metalab.ifmo.ru

Authors

Filipp Komissarenko − *Department of Physics and Engineering, ITMO University, St. Petersburg, Russia*

Ivan Iorsh − *Department of Physics and Engineering, ITMO University, St. Petersburg, Russia*

Dmitry Permyakov − *Department of Physics and Engineering, ITMO University, St. Petersburg, Russia*; orcid.org/0000-0003-2708-9140

Anton Samusev − *Department of Physics and Engineering, ITMO University, St. Petersburg, Russia*; orcid.org/0000-0002-3547-6573

Andrey Bogdanov − *Department of Physics and Engineering, ITMO University, St. Petersburg, Russia*; orcid.org/0000-0002-8215-0445

Complete contact information is available at:
https://pubs.acs.org/10.1021/acsphotonics.9b01515

Notes

The authors declare no competing financial interest.

ACKNOWLEDGMENTS

Numerical and analytical calculations and experimental studies were supported by the Russian Science Foundation (Project No. 19-72-10086). Transfer of silicon nanoparticles on gold substrate was supported by the Russian Science Foundation (Project No. 19-79-00313).

REFERENCES

(1) Kuznetsov, A. I.; Miroshnichenko, A. E.; Fu, Y. H.; Zhang, J.; Luk'yanchuk, B. Magnetic light. *Sci. Rep.* **2012**, *2*, 492.

(2) Evlyukhin, A. B.; Novikov, S. M.; Zywietz, U.; Eriksen, R. L.; Reinhardt, C.; Bozhevolnyi, S. I.; Chichkov, B. N. Demonstration of magnetic dipole resonances of dielectric nanospheres in the visible region. *Nano Lett.* **2012**, *12*, 3749−3755.

(3) Kuznetsov, A. I.; Miroshnichenko, A. E.; Brongersma, M. L.; Kivshar, Y. S.; Luk'yanchuk, B. Optically resonant dielectric nanostructures. *Science* **2016**, *354*, aag2472.

(4) Staude, I.; Schilling, J. Metamaterial-inspired silicon nanophotonics. *Nat. Photonics* **2017**, *11*, 274.

(5) Garcia-Etxarri, A.; Gómez-Medina, R.; Froufe-Perez, L. S.; Lopez, C.; Chantada, L.; Scheffold, F.; Aizpurua, J.; Nieto-Vesperinas, M.; Sáenz, J. J. Strong magnetic response of submicron silicon particles in the infrared. *Opt. Express* **2011**, *19*, 4815−4826.

(6) Shcherbakov, M. R.; Neshev, D. N.; Hopkins, B.; Shorokhov, A. S.; Staude, I.; Melik- Gaykazyan, E. V.; Decker, M.; Ezhov, A. A.; Miroshnichenko, A. E.; Brener, I. Enhanced third-harmonic generation in silicon nanoparticles driven by magnetic response. *Nano Lett.* **2014**, *14*, 6488−6492.

(7) Rybin, M. V.; Koshelev, K. L.; Sadrieva, Z. F.; Samusev, K. B.; Bogdanov, A. A.; Limonov, M. F.; Kivshar, Y. S. High-Q supercavity modes in subwavelength dielectric resonators. *Phys. Rev. Lett.* **2017**, *119*, 243901.

(8) Carletti, L.; Koshelev, K.; De Angelis, C.; Kivshar, Y. Giant nonlinear response at the nanoscale driven by bound states in the continuum. *Phys. Rev. Lett.* **2018**, *121*, 033903.

(9) Fu, Y. H.; Kuznetsov, A. I.; Miroshnichenko, A. E.; Yu, Y. F.; Luk'yanchuk, B. Directional visible light scattering by silicon nanoparticles. *Nat. Commun.* **2013**, *4*, 1527.

(10) Liu, W.; Kivshar, Y. S. Generalized Kerker effects in nanophotonics and meta-optics. *Opt. Express* **2018**, *26*, 13085−13105.

(11) Decker, M.; Staude, I.; Falkner, M.; Dominguez, J.; Neshev, D. N.; Brener, I.; Pertsch, T.; Kivshar, Y. S. High-efficiency dielectric Huygens' surfaces. Advanced. *Adv. Opt. Mater.* **2015**, *3*, 813−820.

(12) Krasnok, A. E.; Simovski, C. R.; Belov, P. A.; Kivshar, Y. S. Superdirective dielectric nanoantennas. *Nanoscale* **2014**, *6*, 7354−7361.

(13) Papasimakis, N.; Fedotov, V.; Savinov, V.; Raybould, T.; Zheludev, N. Electromagnetic toroidal excitations in matter and free space. *Nat. Mater.* **2016**, *15*, 263.

(14) Luk'yanchuk, B.; Paniagua-Domínguez, R.; Kuznetsov, A. I.; Miroshnichenko, A. E.; Kivshar, Y. S. Hybrid anapole modes of high-index dielectric nanoparticles. *Phys. Rev. A: At., Mol., Opt. Phys.* **2017**, *95*, 063820.

(15) Sinev, I. S.; Bogdanov, A. A.; Komissarenko, F. E.; Frizyuk, K. S.; Petrov, M. I.; Mukhin, I. S.; Makarov, S. V.; Samusev, A. K.; Lavrinenko, A. V.; Iorsh, I. V. Chirality driven by magnetic dipole response for demultiplexing of surface waves. *Laser & Photonics Reviews* **2017**, *11*, 1700168.

(16) Picardi, M. F.; Zayats, A. V.; Rodríguez-Fortuño, F. J. Janus and huygens dipoles: near-field directionality beyond spin-momentum locking. *Phys. Rev. Lett.* **2018**, *120*, 117402.

(17) Bliokh, K. Y.; Rodríguez-Fortuño, F. J.; Nori, F.; Zayats, A. V. Spin-orbit interactions of light. *Nat. Photonics* **2015**, *9*, 796.

(18) Mueller, J. B.; Capasso, F. Asymmetric surface plasmon polariton emission by a dipole emitter near a metal surface. *Phys. Rev. B: Condens. Matter Mater. Phys.* **2013**, *88*, 121410.

(19) Aiello, A.; Banzer, P.; Neugebauer, M.; Leuchs, G. From transverse angular momentum to photonic wheels. *Nat. Photonics* **2015**, *9*, 789.

(20) Shitrit, N.; Bretner, I.; Gorodetski, Y.; Kleiner, V.; Hasman, E. Optical spin Hall effects in plasmonic chains. *Nano Lett.* **2011**, *11*, 2038−2042.

(21) Ling, X.; Zhou, X.; Huang, K.; Liu, Y.; Qiu, C.-W.; Luo, H.; Wen, S. Recent advances in the spin Hall effect of light. *Rep. Prog. Phys.* **2017**, *80*, 066401.

(22) Lee, S.-Y.; Lee, I.-M.; Park, J.; Oh, S.; Lee, W.; Kim, K.-Y.; Lee, B. Role of magnetic induction currents in nanoslit excitation of surface plasmon polaritons. *Phys. Rev. Lett.* **2012**, *108*, 213907.

(23) Rodríguez-Fortuño, F. J.; Marino, G.; Ginzburg, P.; O'Connor, D.; Martínez, A.; Wurtz, G. A.; Zayats, A. V. Near-field interference for the unidirectional excitation of electromagnetic guided modes. *Science* **2013**, *340*, 328−330.

(24) Lodahl, P.; Mahmoodian, S.; Stobbe, S.; Rauschenbeutel, A.; Schneeweiss, P.; Volz, J.; Pichler, H.; Zoller, P. Chiral quantum optics. *Nature* **2017**, *541*, 473.

(25) Rodríguez-Fortuño, F. J.; Engheta, N.; Martínez, A.; Zayats, A. V. Lateral forces on circularly polarizable particles near a surface. *Nat. Commun.* **2015**, *6*, 8799.

(26) Picardi, M. F.; Neugebauer, M.; Eismann, J. S.; Leuchs, G.; Banzer, P.; Rodríguez-Fortuño, F. J.; Zayats, A. V. Experimental demonstration of linear and spinning Janus dipoles for polarisation- and wavelength-selective near-field coupling. *Light: Sci. Appl.* **2019**, *8*, 52.

(27) Araneda, G.; Walser, S.; Colombe, Y.; Higginbottom, D. B.; Volz, J.; Blatt, R.; Rauschenbeutel, A. Wavelength-scale errors in optical localization due to spin-orbit coupling of light. *Nat. Phys.* **2019**, *15*, 17−21.

(28) Neugebauer, M.; Banzer, P.; Nechayev, S. Emission of circularly polarized light by a linear dipole. *Sci. Adv.* **2019**, *5*, eaav7588.

(29) Wei, L.; Rodríguez-Fortuño, F. J. Momentum-space geometric structure of helical evanescent waves and its implications on near-field directionality. *Phys. Rev. Appl.* **2020**, *13*, 014008.

(30) Poshakinskiy, A. V.; Poddubny, A. N. Optomechanical Kerker Effect. *Phys. Rev. X* **2019**, *9*, 011008.

(31) Spitzer, F.; Poddubny, A. N.; Akimov, I. A.; Sapega, V. F.; Klompmaker, L.; Kreilkamp, L. E.; Litvin, L. V.; Jede, R.; Karczewski, G.; Wiater, M.; Wojtowicz, T.; Yakovlev, D. R.; Bayer, M. Routing the emission of a near-surface light source by a magnetic field. *Nat. Phys.* **2018**, *14*, 1043−1048.
(32) Neugebauer, M.; Woźniak, P.; Bag, A.; Leuchs, G.; Banzer, P. Polarization-controlled directional scattering for nanoscopic position sensing. *Nat. Commun.* **2016**, *7*, 11286.
(33) Eismann, J. S.; Neugebauer, M.; Banzer, P. Exciting a chiral dipole moment in an achiral nanostructure. *Optica* **2018**, *5*, 954−959.
(34) Harrington, R. On the gain and beamwidth of directional antennas. *IRE Trans. Antennas Propag.* **1958**, *6*, 219−225.
(35) Miroshnichenko, A. E.; Evlyukhin, A. B.; Kivshar, Y. S.; Chichkov, B. N. Substrate-Induced Resonant Magnetoelectric Effects for Dielectric Nanoparticles. *ACS Photonics* **2015**, *2*, 1423−1428.
(36) Dmitriev, P.; Makarov, S.; Milichko, V.; Mukhin, I.; Gudovskikh, A.; Sitnikova, A.; Samusev, A.; Krasnok, A.; Belov, P. Laser fabrication of crystalline silicon nanoresonators from an amorphous film for low-loss all-dielectric nanophotonics. *Nanoscale* **2016**, *8*, 5043−5048.
(37) Denisyuk, A. I.; Komissarenko, F. E.; Mukhin, I. S. Electrostatic pick-and-place micro/nanomanipulation under the electron beam. *Microelectron. Eng.* **2014**, *121*, 15−18.
(38) Renaut, C.; Lang, L.; Frizyuk, K.; Timofeeva, M.; Komissarenko, F. E.; Mukhin, I. S.; Smirnova, D.; Timpu, F.; Petrov, M.; Kivshar, Y.; Grange, R. Reshaping the Second-Order Polar Response of Hybrid Metal-Dielectric Nanodimers. *Nano Lett.* **2019**, *19*, 877−884.
(39) García-Cámara, B.; de La Osa, R. A.; Saiz, J.; González, F.; Moreno, F. Directionality in scattering by nanoparticles: Kerker's null-scattering conditions revisited. *Opt. Lett.* **2011**, *36*, 728−730.
(40) Neugebauer, M.; Bauer, T.; Banzer, P.; Leuchs, G. Polarization tailored light driven directional optical nanobeacon. *Nano Lett.* **2014**, *14*, 2546−2551.
(41) Makarov, S.; Kudryashov, S.; Mukhin, I.; Mozharov, A.; Milichko, V.; Krasnok, A.; Belov, P. Tuning of magnetic optical response in a dielectric nanoparticle by ultrafast photoexcitation of dense electron-hole plasma. *Nano Lett.* **2015**, *15*, 6187−6192.
(42) de Galarreta, C. R.; Sinev, I.; Alexeev, A. M.; Trofimov, P.; Ladutenko, K.; Carrillo, S. G.-C.; Gemo, E.; Baldycheva, A.; Nagareddy, V. K.; Bertolotti, J. All-Dielectric Silicon/Phase-Change Optical Metasurfaces with Independent and Reconfigurable Control of Resonant Modes. *arXiv:1901.04955 [physics.optics]* **2019**, na.
(43) Komar, A.; Paniagua-Dominguez, R.; Miroshnichenko, A.; Yu, Y. F.; Kivshar, Y. S.; Kuznetsov, A. I.; Neshev, D. Dynamic beam switching by liquid crystal tunable dielectric metasurfaces. *ACS Photonics* **2018**, *5*, 1742−1748.

https://dx.doi.org/10.1021/acsphotonics.9b01515
ACS Photonics 2020, 7, 680−686